NeuroToxicology 63 (2017) 70–83

Contents lists available at ScienceDirect

NeuroToxicology

Full Length Article

Time-dependent effects of perfluorinated compounds on viability in cerebellar granule neurons: Dependence on carbon chain length and functional group attached

Hanne Friis Berntsen[a,b,*,1], Cesilie Granum Bjørklund[a], Jean-Nicolas Audinot[c], Tim Hofer[d], Steven Verhaegen[a], Esther Lentzen[c], Arno Christian Gutleb[e], Erik Ropstad[a]

[a] Department of Production Animal Clinical Sciences, NMBU-School of Veterinary Science, P.O. Box 8146 Dep, N-0033, Oslo, Norway
[b] Department of Administration, Lab Animal Unit, National Institute of Occupational Health, P.O. Box 8149 Dep, N-0033, Oslo, Norway
[c] Materials Research and Technology (MRT) Department, Luxembourg Institute of Science and Technology (LIST), 5 avenue des Hauts-Fourneaux, Esch-sur-Alzette, Luxembourg
[d] Department of Toxicology and Risk Assessment, Infection Control and Environmental Health, Norwegian Institute of Public Health, P.O. Box 4404 Nydalen, N-0403, Oslo, Norway
[e] Environmental Research and Innovation (ERIN) Department, Luxembourg Institute of Science and Technology (LIST), 5 avenue des Hauts-Fourneaux, Esch-sur-Alzette, Luxembourg

ARTICLE INFO

Article history:
Received 15 March 2017
Received in revised form 11 August 2017
Accepted 12 September 2017
Available online 15 September 2017

Keywords:
Perfluoroalkyl and polyfluoroalkyl acids
Carbon chain length
Cytotoxicity
Cerebellar granule cells
Nano secondary ion mass spectrometry
Lipid peroxidation

ABSTRACT

The toxicity of long chained perfluoroalkyl acids (PFAAs) has previously been reported to be related to the length of the perfluorinated carbon chain and functional group attached. In the present study, we compared the cytotoxicity of six PFAAs, using primary cultures of rat cerebellar granule neurons (CGNs). Two perfluoroalkyl sulfonic acids (PFSAs, chain length C_6 and C_8) and four perfluoroalkyl carboxylic acids (PFCAs, chain length C_8–C_{11}) were studied. These PFAAs have been detected in human blood and the brain tissue of mammals. The cell viability trypan blue and MTT assays were used to determine toxicity potencies (based on LC_{50} values) after 24 h exposure (in descending order): perfluoroundecanoic acid (PFUnDA) ≥ perfluorodecanoic acid (PFDA) > perfluorooctanesulfonic acid potassium salt (PFOS) > perfluorononanoic acid (PFNA) > perfluorooctanoic acid (PFOA) > perfluorohexanesulfonic acid potassium salt (PFHxS). Concentrations of the six PFAAs that produced equipotent effects after 24 h exposure were used to further explore the dynamics of viability changes during this period. Therefore viability was assessed at 10, 30, 60, 90, 120 and 180 min as well as 6, 12, 18 and 24 h. A difference in the onset of reduction in viability was observed, occurring relatively quickly (30–60 min) for PFOS, PFDA and PFUnDA, and much slower (12–24 h) for PFHxS, PFOA and PFNA. A slight protective effect of vitamin E against PFOA, PFNA and PFOS-induced reduction in viability indicated a possible involvement of oxidative stress. PFOA and PFOS did not induce lipid peroxidation on their own, but significantly accelerated cumene hydroperoxide-induced lipid peroxidation. When distribution of the six PFAAs in the CGN-membrane was investigated using NanoSIMS50 imaging, two distinct patterns appeared. Whereas PFHxS, PFOS and PFUnDA aggregated in large hotspots, PFOA, PFNA and PFDA showed a more dispersed distribution pattern. In conclusion, the toxicity of the investigated PFAAs increased with increasing carbon chain length. For molecules with a similar chain length, a sulfonate functional group led to greater toxicity than a carboxyl group.

1. Introduction

Per- and polyfluoroalkyl substances (PFASs) may be defined as aliphatic substances on which one or several (poly-) or all (per-) C atoms in the carbon chain have had their H atoms substituted by F atoms (Buck et al., 2011). PFASs have been used in industrial and consumer products since the 1950s, resulting due to their high stability in widespread contamination of the environment,

* Corresponding author at: Department of Production Animal Clinical Sciences, NMBU-School of Veterinary Science, P.O. Box 8146 Dep, N-0033, Oslo, Norway.
E-mail addresses: Hanne.Berntsen@stami.no, hanne.friis.berntsen@nmbu.no (H.F. Berntsen).
[1] URL: http://www.nmbu.no/en .

https://doi.org/10.1016/j.neuro.2017.09.005
0161-813X/

including humans and wildlife (Buck et al., 2011). However, only in the early 2000s awareness was raised regarding the issue of environmental contamination. Perfluorooctanesulfonic acid (PFOS), perfluorooctanoic acid (PFOA) and other PFASs were then detected in human blood samples (Buck et al., 2011; Hansen et al., 2001), as well as PFOS in samples from wildlife (Buck et al., 2011; Giesy and Kannan, 2001). Since investigations on the effects of PFASs started, an increasing number of *in vivo* and *in vitro* studies report effects related to the nervous system.

A subgroup of the PFASs are the perfluoroalkyl acids (PFAAs), which include the perfluoroalkyl carboxylic acids (PFCAs) and perfluoroalkyl sulfonic acids (PFSAs). These are often divided into short- or long-chained compounds. Long-chained compounds involve molecules with eight or more carbon atoms in the chain (or seven perfluorinated C-atoms) for PFCAs, and six or more carbon atoms in the chain for PFSAs (Buck et al., 2011; OECD, 2016). This distinction is based on differences in their toxicity and tendency to bioconcentrate and bioaccumulate (Martin et al., 2003a,b). For the long chained PFAAs toxicity or adverse effects are reported to increase with carbon chain length in various cell culture models (Kleszczynski et al., 2007; Liao et al., 2009; Mulkiewicz et al., 2007) as well as zebrafish embryos (Hagenaars et al., 2011), and is related to the functional group attached (Gorrochategui et al., 2014; Hagenaars et al., 2011; Liao et al., 2009). Yet other studies fail to find such a connection, e.g. Halsne et al. (2016) observed an increase in cell death in monolayers of MCF-10A cells after exposure to PFOS and perfluorodecanoic acid (PFDA), but not after exposure to perfluoroundecanoic acid (PFUnDA). In the same study, PFOS, perfluorononanoic acid (PFNA) and PFDA led to abnormal acini development in 3D cultures of these cells, whereas PFOA and PFUnDA had little or no effect at equimolar concentrations.

In adult rodents, exposure to PFAAs has been associated with altered concentrations of neurotransmitters in the brain (Yu et al., 2016), and increased sensitivity to induced convulsions (Sato et al., 2009). Neonatal exposures of mice to PFOS and PFOA have been reported to affect proteins important in neuronal growth and synaptogenesis in the developing brain, and result in neurobehavioural effects in adults (Johansson et al., 2009, 2008). Roth and Wilks (2014) critically reviewed human epidemiological studies up to 2014, associating exposure to perfluorinated chemicals with neurodevelopmental and/or neurobehavioural effects in infants and children. Although, they concluded that at present the evidence did not support a strong causal association, much due to large variability between the studies, they advocated future studies with larger study populations and a more harmonised study design. More recently, another study suggested prenatal exposure to PFOS and PFOA may have a small to moderate effect on children's neuro-behavioural development, specifically in terms of hyperactive behaviour (Hoyer et al., 2015).

The PFSAs perfluorohexanesulfonic acid (PFHxS) and PFOS as well as the PFCAs PFOA, PFNA, PFDA and PFUnDA have long elimination half-lives in humans (Haug et al., 2010a; Holzer et al., 2009; Nilsson et al., 2010; Olsen et al., 2007). PFAAs do not accumulate preferentially in fat, but bind to proteins such as plasma proteins, and proteins in the liver (OECD, 2002). All the six above-mentioned compounds are found in significant concentrations in human blood samples (Haug et al., 2010b; Karrman et al., 2007). Further, they have been detected in wildlife, including the brain of harbour seals (Ahrens et al., 2009), as well as in brains from polar bears (Eggers Pedersen et al., 2015; Greaves et al., 2013). This indicates that the PFAAs do cross the blood-brain barrier and reach measurable concentrations in the brain after environmental exposure. In a study by Maestri et al. (2006) PFOS and PFOA were also measured and detected in human brains.

Reactive oxygen species (ROS) are products of normal metabolism in the cell in the presence of oxygen, and are mostly produced through oxidative metabolism in mitochondria, enzymatic mixed-function oxidation reactions, and autoxidation of small molecules (Simonian and Coyle, 1996). The formation of ROS in the body is counterbalanced by antioxidant defence systems (Halliwell, 1997), which if overwhelmed may result in oxidative stress, potentially causing cellular dysfunction or cell death, because of damage to molecules such as lipids, proteins and DNA (Simonian and Coyle, 1996). The brain is especially prone to damage from oxidative stress, due to the presence of high levels of oxygen, poor anti-oxidant defence systems, high levels of polyunsaturated fatty acids in the cell membrane, and a high content of iron in certain brain areas (Mariussen et al., 2002; Sayre et al., 2008). A study by Reistad et al. (2013) indicated that PFASs can induce ROS in cultured cerebellar granule neurons. Formation of ROS may in turn induce lipid peroxidation, a process in which lipids containing carbon–carbon double bonds, and in particular those of polyunsaturated fatty acids, are attacked (Ayala et al., 2014), resulting in the generation of other harmful reactive species (Hofer et al., 2014). Lipid peroxidation has been associated with neurodegenerative diseases such as Alzheimer's disease and Parkinson's disease (Sayre et al., 2008).

Long chained PFAAs such as PFOS and PFOA as well as perfluorododecanoic acid (PFDoDA) and perfluorotridecanoic acid (PFTrDA) have been found to partition into lipid bilayers. (Lehmler and Bummer, 2004; Xie et al., 2010a, 2010b). With Nano Secondary Ion Mass Spectrometry (NanoSIMS50), it is possible to measure and map the distribution of up to five isotopes simultaneously in biological material on a nanometre scale (50 nm resolution). This technique is a powerful tool to elucidate localisation of halogenated compounds (among others) on the cell membrane and in tissues, as previously shown (Audinot et al., 2013; Georgantzopoulou et al., 2013; Gutleb et al., 2012). In this study we have applied it to evaluate distribution of the different PFAAs at the surface of the cell membrane in exposed cultures of cerebellar granule neurons (CGNs).

Most published studies on PFAAs, also in neuronal cultures, focus on PFOS and PFOA, whereas fewer studies have been conducted with PFHxS, PFNA, PFDA and PFUnDA. Interestingly, in a recent study, the dominating PFAAs in polar bear brains were in addition to PFOS the longer chained PFUnDA, PFDoDA and PFTrDA (Eggers Pedersen et al., 2015). Studies investigating whether these compounds are more toxic than shorter chained and less prominent equivalents, are therefore of importance. In the same study, the second highest mean concentrations of PFAAs were detected in the cerebellum, only exceeded by levels in the brain stem. Granule cells are the most abundant neurons in the cerebellum (Gallo et al., 1982), are easy to isolate, and are suitable for *in vitro* studies.

In the present study on isolated rat CGNs, the aim was to investigate whether the overall toxicity of six long chained PFAAs, is dependent on carbon chain length as well as the functional group attached. The time-dependent changes in viability were also assessed. We focused on the two PFSAs PFHxS and PFOS, as well as the PFCAs PFOA, PFNA, PFDA and PFUnDA in the experiments due to their detectable levels in human blood samples and brain samples from wildlife. The toxicity of these six compounds has not previously been compared in cerebellar neuronal cultures. In addition to effects on viability, we wanted to investigate the involvement of ROS production and lipid peroxidation in PFAA-induced neuronal toxicity. Finally, we sought to assess whether the differences in chain length and functional group could be related to the distribution pattern of the PFAAs on the cell membrane.

2. Animals, materials and methods

2.1. Chemicals and reagents

Albumin from bovine serum (BSA, ≥ 96%), α-tocopherol (vitamin E), cumene hydroperoxide (cumOOH, 6 M), cytosine β-D-arabinofuranoside (ARA-C), deoxyribonuclease I from bovine pancreas (DNAse), dimethyl sulfoxide (DMSO, ≥99.9%), perfluorooctanesulfonic acid potassium salt (PFOS ≥ 98%), perfluorooctanoic acid (PFOA, 96%), perfluorononanoic acid (PFNA, 97%), perfluorodecanoic acid (PFDA, 98%) perfluoroundecanoic acid (PFUnDA, 95%), poly-L-lysine hydrobromide (M_w > 70,000 g/mol), 3-(4,5-dimethylthiazol-2-yl)-2,5-diphenyl tetrazolium bromide (MTT), trypan blue solution (0.4%), trypsin (type I) from bovine pancreas and trypsin inhibitor from glycine max (soybean type I-S) were purchased from Sigma-Aldrich, St. Louis, MO, USA. Tridecafluorohexane-1-sulfonic acid potassium salt (PFHxS, > 98%) was from Santa Cruz Biotechnology, Inc, Santa Cruz, CA, USA. Basal medium Eagle (BME), C_{11}-BODIPY, 2′,7′- dichlorodihydrofluorescein diacetate (DCFH-DA), Dulbecco's Phosphate-Buffered Saline (DPBS) with calcium and magnesium, heat inactivated foetal bovine serum (FBS), Glutamax-I supplement – 200 mM, Hanks' Balanced Salt Solution (HBSS) – 10X, HEPES buffer – 1 M and penicillin-streptomycin 100 IU/ml penicillin and 100 μg/ml streptomycin were obtained from GIBCO/Invitrogen, Norway. Acetone – analysis-grade, came from Merck Millipore, Munich, Germany, whereas H_2O_2 was purchased from Norsk Medisinaldepot AS, Oslo, Norway. Osmium tetroxide, crystalline (> 99.95%) was delivered by Electron Microscopy Sciences, Hatfield, PA, USA, and glutaraldehyde from Taab Laboratory Equipment Ltd., Reading, UK. All other chemicals and reagents used were obtained from standard commercial suppliers. Stock solutions of C_{11}-BODIPY, DCFH-DA, all relevant concentrations of PFAAs and vitamin E were prepared by dissolution in DMSO, frozen, and thawed before each experiment. The chemical structures of the six PFAAs used are presented in Fig. 1.

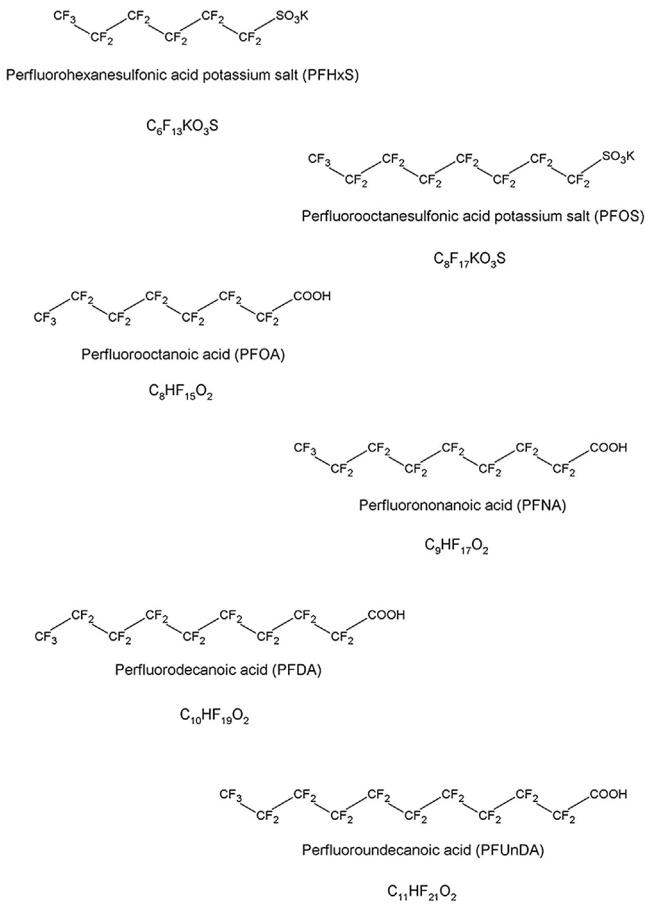

Fig. 1. The chemical structures of the six different PFAAs.

2.2. Laboratory animals

For each isolation of cells, a mixed-sex litter of 10 Wistar rat pups was obtained at 8 days of age from Taconic, Denmark. The pups were euthanised, without prior use of anaesthesia, by decapitation on the day of arrival, whereas the mother was anaesthetised with isoflurane (2.5% ISO and 250 ml airflow) before euthanasia with an intracardiac injection of pentobarbital. All animal treatments were carried out at the Animal Laboratory Unit at the Section of Experimental Biomedicine, Norwegian University of Life Sciences (Oslo) and were in accordance with the Norwegian Animal Welfare Act and the Directive 2010/63/EU of the European Parliament and of the Council on the protection of animals used for scientific purposes. Efforts were made to minimise animal suffering and to reduce the number of animals used.

2.3. Isolation of cerebellar granule neurons

Primary cultures of post-mitotic CGNs were prepared as described in Berntsen et al. (2013) from 8-day-old rat pups. Cells from each isolation were obtained from the pooled cerebella of 10 animals, diluted to an approximate concentration of 1-1.2 × 10^6 cells/ml. Cells were cultured in BME, supplemented with 10% heat-inactivated FBS, 2.5 mM Glutamax, 100 IU/ml penicillin + 100 μg/ml streptomycin, 25 mM KCl and 1% glucose. Diluted cells were transferred to 12-well Nunc-cell-culture plates (GIBCO/Invitrogen, 1 ml cells per well) pre-coated with poly-L-lysine (0.01 mg/ml for 2 h, 1 ml per well) for the cytotoxicity experiments. For the NanoSIMS imaging, cells were seeded at the same concentration in 12-well plates containing poly-L-lysine coated silica wafers (Siltronix, Archamps, France). For the assessment of ROS production as well as lipid peroxidation, cells were seeded on poly-L-lysine coated black, clear bottom, 96-well plates (Corning®, Costar®, Sigma-Aldrich, 125 μl cells per well). To prevent the replication of non-neuronal cells, the cytostatic drug ARA-C was added to all plates after 24 h – on day 1 *in vitro* (DIV), giving a concentration of 10.3 μM in the cell medium. Cells were then left undisturbed in a CO_2 incubator at 36 °C and 5% CO_2 until DIV 7 or 8, when exposures were carried out. Cultures of CGNs typically contains 80–90% granule cells, and 5–10% glial cells (Drejer et al., 1982). A representative image of a neuronal culture from DIV 5 is presented in Fig. 2.

2.4. Cell viability assays

2.4.1. The MTT assay

The 3-(4,5-dimethylthiazol-2-yl)-2,5-diphenyl tetrazolium bromide (MTT) assay is based on the cleavage of the yellow tetrazolium salt MTT into the blue product formazan by the mitochondrial enzyme succinate dehydrogenase in living cells (Mosmann, 1983). In the assay, a decrease in the number of living cells results in a reduction of the amount of formazan produced as compared to the control, and indicates the degree of cytotoxicity induced. The assay was executed as described in Berntsen et al. (2013). Dual wavelength absorbance measurements were performed at 570 and 690 nm in a VICTOR3 multilabel reader (PerkinElmer, Inc. Waltham, MA, USA).

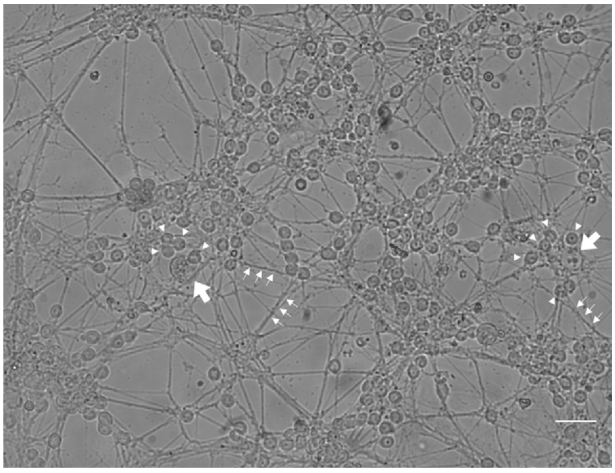

Fig. 2. A representative light microscope image of a cerebellar neuronal culture taken at 5 days *in vitro*. The neurons were isolated from 8 day old rat pups. Cerebellar granule neurons (arrowheads) typically aggregate in loose clusters, sometimes in association with remaining glial cells (broad arrow). The granule cells extend a dense interconnecting network of neurite outgrowths (small arrows). Scale bar = 20 μm.

2.4.2. The trypan blue assay

The trypan blue exclusion assay is based on the staining of dead or damaged cells due to uptake of dye through leaky cell membranes, and the exclusion of dye by viable cells with intact cell membranes (Louis and Siegel, 2011). For the trypan blue assay, cells were stained after the following protocol: medium covering CGNs was gently removed, before cells were washed with DPBS, and stained with 0.4% trypan blue (300 μl/dish) for 10 min at room temperature. Subsequently, the trypan blue solution was removed and cells washed once with DPBS, which was thereafter replaced by fresh DPBS before cells were immediately counted using a light microscope. The number of trypan blue positive cells per 100 cells were counted in three random areas of each dish, from which an average value was calculated for each dish.

2.5. PFAA exposure and assessment of cytotoxicity

2.5.1. Concentration-response assessment

For the assessment of cytotoxicity after exposure to the different PFAAs, CGNs were exposed at DIV 8 to increasing concentrations of toxicants in BME (1 ml/well) supplemented with 2.5 mM Glutamax, 100 IU/ml penicillin + 100 μg/ml streptomycin, 25 mM KCl and 1% glucose, without FBS. A mean value was calculated for each exposure, performed in triplicate wells on the same plate or in 3 dishes for 24 h. In all cell viability experiments described in the present paper an unexposed medium control as well as a DMSO control (0.1-0.2%) were included, and the calculated mean values for the different exposures in each experiment were expressed as % viability compared to the DMSO control (given a value of 100%) from the same experiment. Preliminary range-finding experiments were performed with the MTT assay to make sure that concentrations producing from no to full cytotoxicity were included for the construction of concentration-response curves. Toxicity was initially assessed with the MTT assay (n = 5–8 independent experiments, each from a separate cell isolation, with each condition tested in triplicate wells on the same plate per experiment). The results were thereafter confirmed in further experiments with the trypan blue assays, using the same concentration-interval (n = 3–4 independent experiments, each from a separate cell isolation with each condition tested in three separate dishes per experiment). The concentrations of the various PFAAs used in the MTT and trypan blue assays are presented in Table 1.

Table 1
Concentrations of PFAAs used for cell viability experiments, determined by preliminary range-finding experiments.

Compound	Exposure concentrations μM	
	MTT	Trypan blue
PFHxS	200, 300, 400, 450, 500, 550, 600	200, 300, 400, 450, 500, 600
PFOS	10, 20, 40, 60, 80, 100	10, 20, 40, 60, 80, 100
PFOA	100, 200, 300, 400, 500, 600	100, 200, 300, 400, 500, 600
PFNA	10, 20, 40, 60, 80, 100, 120, 140	10, 20, 40, 80, 100, 120
PFDA	10, 20, 30, 40, 60, 80, 100	10, 20, 30, 40, 60, 80
PFUnDA	5, 10, 15, 20, 30, 40, 60, 80, 100	10, 15, 20, 30, 40, 80

2.5.2. Time-dependent effects on cell viability

To investigate how quickly reductions in cell viability were induced after PFAA exposure, and how the viability did vary over a period of 24 h, CGNs were exposed (on DIV 8) to a single concentration of the 6 different PFAAs for the following time intervals; 10, 30, 60, 90, 120 and 180 min and 6, 12, 18 and 24 h. Cell viability was after end of exposure assessed with the MTT assay (n = 3-4 independent experiments, each from a separate cell isolation, with each condition tested in triplicate wells on the same plate per experiment. A mean value was calculated for the triplicate wells). All time-points were measured in each individual repeat. The concentrations used were chosen based on the concentration-response experiments (Section 3.1). A single concentration of each PFAA producing close to equipotent effects, i.e. some, but not full toxicity (60–80% reduction in cell viability) at 24 h, was selected. For the six PFAAs, the following concentrations were used: 550 μM PFHxS, 60 μM PFOS, 500 μM PFOA, 100 μM PFNA, 40 μM PFDA and 30 μM PFUnDA. At all time points a 0.1% DMSO control as well as an unexposed control (medium only) was also included.

2.5.3. Effects of vitamin E on PFAA-induced cytotoxicity

To get an indication on the involvement of oxidative stress in PFAA-induced cytotoxicity, CGNs were co-incubated with 550 μM PFHxS, 60 μM PFOS, 500 μM PFOA, 100 μM PFNA, 40 μM PFDA or 30 μM PFUnDA and 50 μM of the anti-oxidant vitamin E for 24 h, before cell viability was assessed with the MTT assay (n = 5-7 independent experiments, each from a separate cell isolation, with each condition tested in triplicate wells, on the same plate per experiment. A mean value was calculated for the triplicate wells). The concentration of vitamin E was based on previously published studies (Berntsen et al., 2013; Mariussen et al., 2002; Reistad et al., 2007). The concentrations of the PFAAs were as in the time-dependent assay chosen as they produced some, but not full cytotoxicity at 24 h in the concentration-response studies. Vitamin E was also tested alone to make sure that it did not influence cell viability.

2.6. Assessment of PFAA-induced ROS production and lipid peroxidation

2.6.1. Assessment of ROS production with the DCF-fluorescence assay

For assessment of the production of reactive oxygen species (ROS), CGNs were exposed to 75, 150, 300 and 600 μM PFHxS, PFOS, PFOA, PFNA, PFDA and PFUnDA or 1 mM H_2O_2 (positive control) in supplemented HBSS buffer (pH 7.4) (containing 20 mM HEPES, 4.17 mM $NaHCO_3$, 5 mM glucose and 25 mM KCl) on DIV 7 for three hours, during which ROS production was assessed with the DCF-fluorescence assay (n = 3 independent experiments, each

from a separate cell isolation, with each condition tested in triplicate wells, on the same plate per experiment). All experiments included an unexposed buffer control as well as a DMSO control (0.1%). A mean value was calculated for triplicate wells from each experiment. The DCF assay is based on the diffusion of the non-ionic probe 2′,7′-dichlorodihydrofluorescein diacetate (DCFH-DA) across the cell membrane, and its hydrolysis to the non-fluorescent DCFH inside the cell through the action of intracellular esterases. DCFH may be oxidised to the fluorescent DCF when ROS such as $ONOO^-$, $^{\bullet}OH$, $ROO^{\bullet}$ and H_2O_2/ROOH (in combination with cellular peroxidases or catalytic metal ions) are present (Hofer, 2001; Hofer et al., 2014; Myhre et al., 2003). In brief, the medium from each well of the 96 well plate was rapidly withdrawn, and carefully replaced with 250 μl supplemented HBSS buffer containing 5 μM DCFH-DA. Cells were subsequently incubated in the dark for 20 min at 36 °C and 5% CO_2, before replacement of the DCFH-DA solution with 250 μl of toxicants in HBSS buffer. Fluorescence readings were initiated immediately and continued for 3 h in a VICTOR3 1420 multilabel plate reader (PerkinElmer, Inc. Waltham, MA, USA) at 37 °C. The area under the curve (AUC) was calculated for each well, and values expressed as fluorescence relative to the DMSO control (set to a value of 100).

2.6.2. Assessment of cellular lipid peroxidation using the CLPAA-assay

Lipid peroxidation was assessed using the probe C_{11}-BODIPY (n = 3 independent experiments, each from a separate cell isolation, with each condition tested in triplicate wells, on the same plate per experiment). CGNs were exposed to increasing

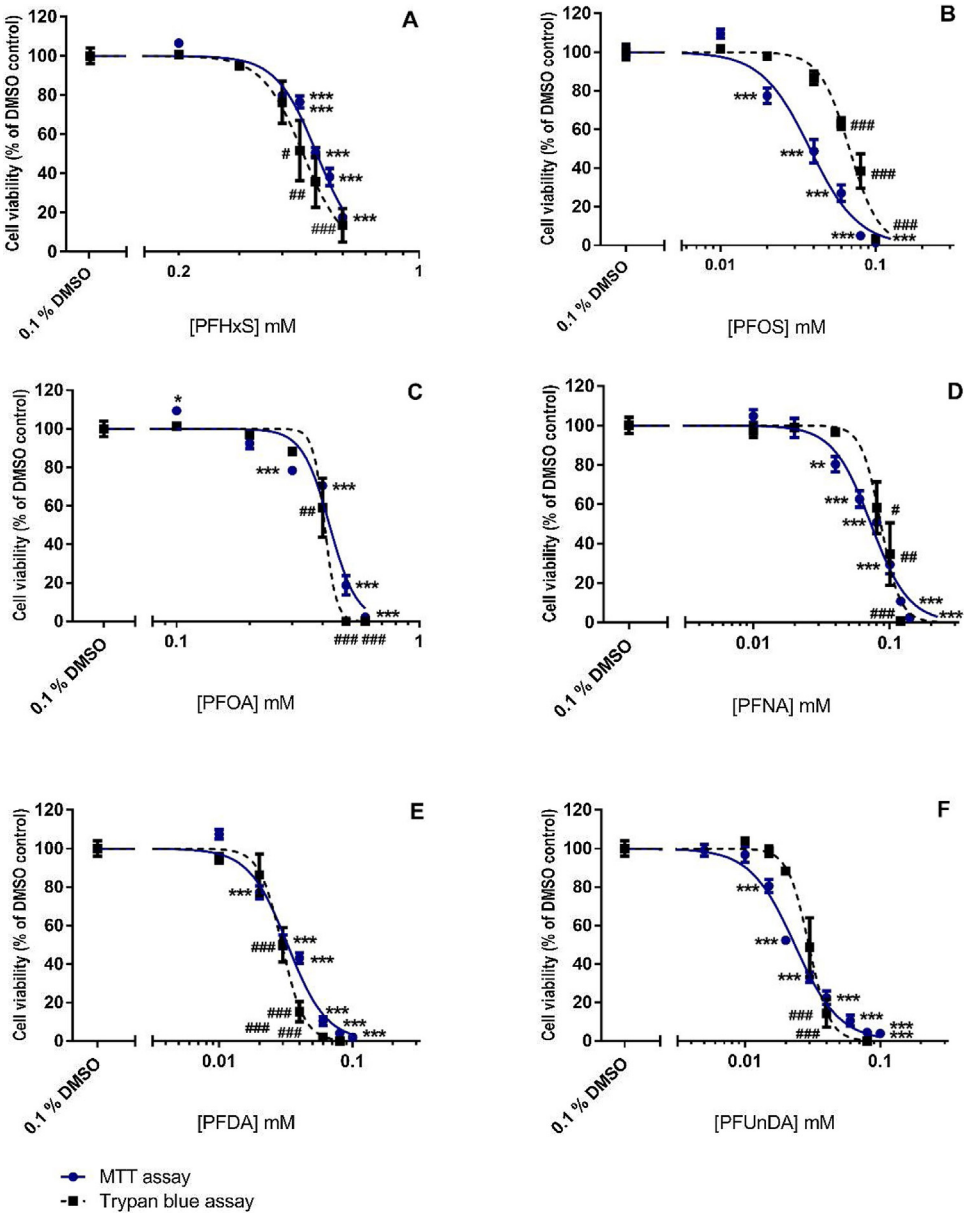

Fig. 3. Concentration dependent reductions in viability of cerebellar granule neurons exposed to increasing concentrations of A) PFHxS, B) PFOS, C) PFOA, D) PFNA, E) PFDA and F) PFUnDA for 24 h. Viability was assessed with the MTT and trypan blue assays. Statistical differences from the 0.1% DMSO control were assessed with ANOVA and Dunnett's post hoc test, with the exception of PFOS (MTT/trypan blue), PFNA (MTT) and PFUnDA (trypan blue), where a Welch's ANOVA with a Games-Howell post hoc test was used. *,**,*** and #,##,### indicate significant differences ($p < 0.05$, $p < 0.01$ and $p < 0.001$) relative to the 0.1% DMSO cell control (defined as 100%), with MTT and trypan blue, respectively. Mean values and SEM are displayed, n = 5-8 independent experiments, each from a separate cell isolation (MTT), and n = 3-4 independent experiments, each from a separate cell isolation (trypan blue), with each condition performed in triplicate.

Table 2
NOEC, LOEC and LC_{50} values in CGNs for the six tested PFAAs assessed with the MTT and trypan blue assays after 24 h exposure.

	MTT μM				Trypan blue μM			
PFAA	NOEC	LOEC	LC_{50}	LC_{50} 95% CI	NOEC	LOEC	LC_{50}	LC_{50} 95% CI
PFHxS	300	400	500	[495,514]	400	450	460	[432,490]
PFOS	10	20	38	[34,42]	40	60	68	[63,73]
PFOA	200	300	427	[411,434]	300	400	408	[391,426]
PFNA	20	40	73	[68,77]	40	80	86	[78,94]
PFDA	10	20	33	[31,34]	20	30	30	[27,32]
PFUnDA	10	15	23	[22,25]	30	40	30	[27,32]

NOEC – No observed effect concentration.
LOEC – Lowest observed effect concentration.
LC_{50} – Lethal concentration killing 50% of the cells.
CI – Confidence interval.
PFAA – Perfluoroalkyl acid, PFHxS – perfluorohexanesulfonic acid, PFOS – perfluorooctanesulfonic acid, PFOA – perfluorooctanoic acid, PFNA – perfluorononanoic acid, PFDA – perfluorodecanoic acid, PFUnDA – perfluoroundecanoic acid.

concentrations of PFOS (10, 20, 40, 60, 80, 100 μM), PFOA (100, 200, 300, 400, 500, 600 μM), 0.1% DMSO or supplemented HBSS buffer only on DIV 7, in the presence or absence of the lipid peroxidation-inducer cumene hydroperoxide (cumOOH). The same concentrations of PFOS and PFOA as tested in the 24 h MTT cytotoxicity assay were used. The method used in the present study was based on the cellular lipid peroxidation antioxidant assay (CLPAA) as described by Hofer et al. (2014) with slight modifications. The CLPAA assay is based on the oxidation of the cell membrane soluble and oxidation sensitive probe C_{11}-BODIPY (which emits natural red fluorescence) by free radicals, to green fluorescent C_{11}-BODIPY oxidation products. The two green fluorescent products created by free radical attack of C_{11}-BODIPY correlates to the amount of lipid peroxidation taking place (Hofer et al., 2014). Lipid peroxidation in cellular membranes is induced by addition of cumOOH, which generates oxidising hydroxyl radicals (•OH) (Hofer et al., 2014). In the present study, we investigated whether PFOS and PFOA were capable of accelerating induced lipid peroxidation in CGNs, and in addition assessed whether exposure to PFOS or PFOA alone, would affect the background lipid peroxidation rate. Briefly, the medium covering cells was removed from each well of the 96-well plate and replaced with 100 μl of C_{11}-BODIPY (5 μM) in supplemented HBSS. The plate was subsequently incubated for 30 min in the dark at 36 °C and 5% CO_2, before the C_{11}-BODIPY solution was removed, wells washed once with 100 μl HBSS, and replaced with 200 μl of PFOS or PFOA at different concentrations in supplemented HBSS buffer ± cumOOH (50 μM). The plate was thereafter read repeatedly in a CLARIOstar® microplate reader (BMG Labtech, Ortenberg, BW, Germany) at 37 °C for up to 1 h 30 min in the presence of cumOOH and up to 3 h in its absence. For induced lipid peroxidation, the increase in green fluorescence was linear the first hour after addition of cumOOH, and data were fitted using linear regression with calculation of slopes using CLARIOstar® MARS 3.00 software. For background lipid peroxidation (no inducer added; the rate of lipid peroxidation was considerably lower compared to when having added the inducer), data between 0 and 3 h were fitted using linear regression.

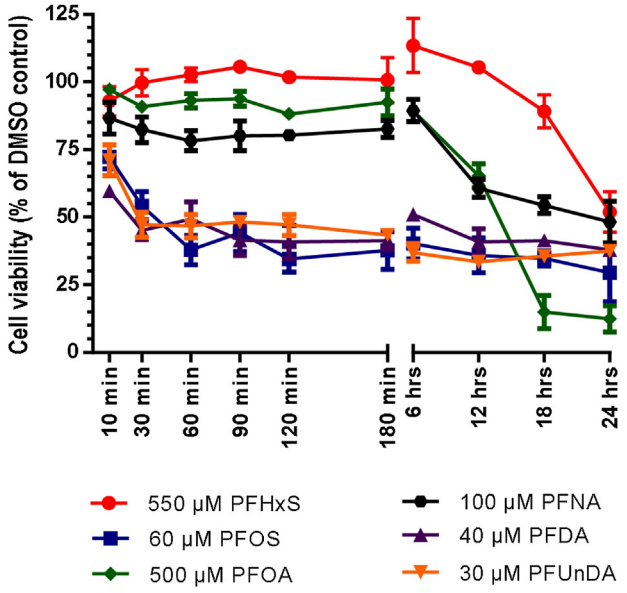

Fig. 4. Time-dependent effects of the six PFAAs on cell viability in cerebellar granule neurons, after exposure to concentrations previously determined to exert equipotent effects at 24 h. Viability was assessed with the MTT assay after exposure of CGNs to 550 μM PFHxS, 60 μM PFOS, 500 μM PFOA, 100 μM PFNA, 40 μM PFDA and 30 μM PFUnDA for 10,30,60,90,120 and 180 min, and 6, 12, 18 and 24 h. All values are relative to the 0.1% DMSO control (defined as 100%). Mean values and SEM are displayed (n = 3–4 independent experiments, each from a separate cell isolation, with each condition performed in triplicate).

2.7. NanoSIMS imaging

For the examination of the distribution of the PFAAs on the cell membrane, CGNs grown on top of silica wafers were (on DIV 8) exposed for 24 h to equimolar sub-toxic concentrations (10 μM) of the six PFAAs or 0.1% DMSO in supplemented BME, without FBS, before imaging with NanoSIMS 50 (Cameca, Gennevilliers, France). One silica wafer with cells was used per exposure. At the end of exposure, the medium covering the wafers with cells was gently replaced with a 5% glutaraldehyde solution in DPBS supplemented with 25 mM KCl, and left in the fridge overnight. The subsequent day, after removal of the glutaraldehyde solution and 15 min of gentle agitation with supplemented DPBS, fixation with 1% osmium tetroxide (OsO_4) in supplemented DPBS buffer was carried out for 1 h before washing was repeated for 15 min. Subsequently, cells on the wafers were dehydrated using increasing acetone concentrations (30%, 50%, 70%, 90% and 100% acetone), and thereafter left to air dry. During NanoSIMS 50 analyses a focused primary ion beam of Cs^+ ions is rastered across the surface of the sample, and secondary ions generated by sputtering are extracted and analysed according to their respective charge-to-mass ratios at high mass resolving power (Kraft et al., 2006). The samples from the present experiment were analysed without the implantation of Cesium as described in Kraft et al. (2006) and Audinot et al. (2011). The impact of the primary beam used was 16 keV with an intensity of 1.5 pA. Images were recorded in a pixel format of 256 × 256 image points with a counting time of 20 ms per pixel for a raster size of 40 × 40 μm^2 to 55 × 55 μm^2. The probe-working diameter was in the range of 80 nm. The secondary negative ions and clusters recorded simultaneously were: $^{19}F^-$ (m = 18.99840 amu), $^{31}P^-$ (m = 30.97376 amu) and $^{12}C^{14}N^-$ (m = 26.00307 amu). Images of several cells were recorded for each exposure. The signals were simultaneously collected with independent electron multipliers. Fluorine images visualise the localisation of the perfluorinated compounds. The phosphorus images allow to localise the membrane and the genetic information (phospholipids, DNA, nucleus). Ubiquitous carbon and nitrogen atoms that recombine to CN-ions provide pictures of the cell morphology similar to those obtained with optical microscopy (signal assimilated to the proteins) (Audinot et al., 2013; Georgantzopoulou et al., 2013).

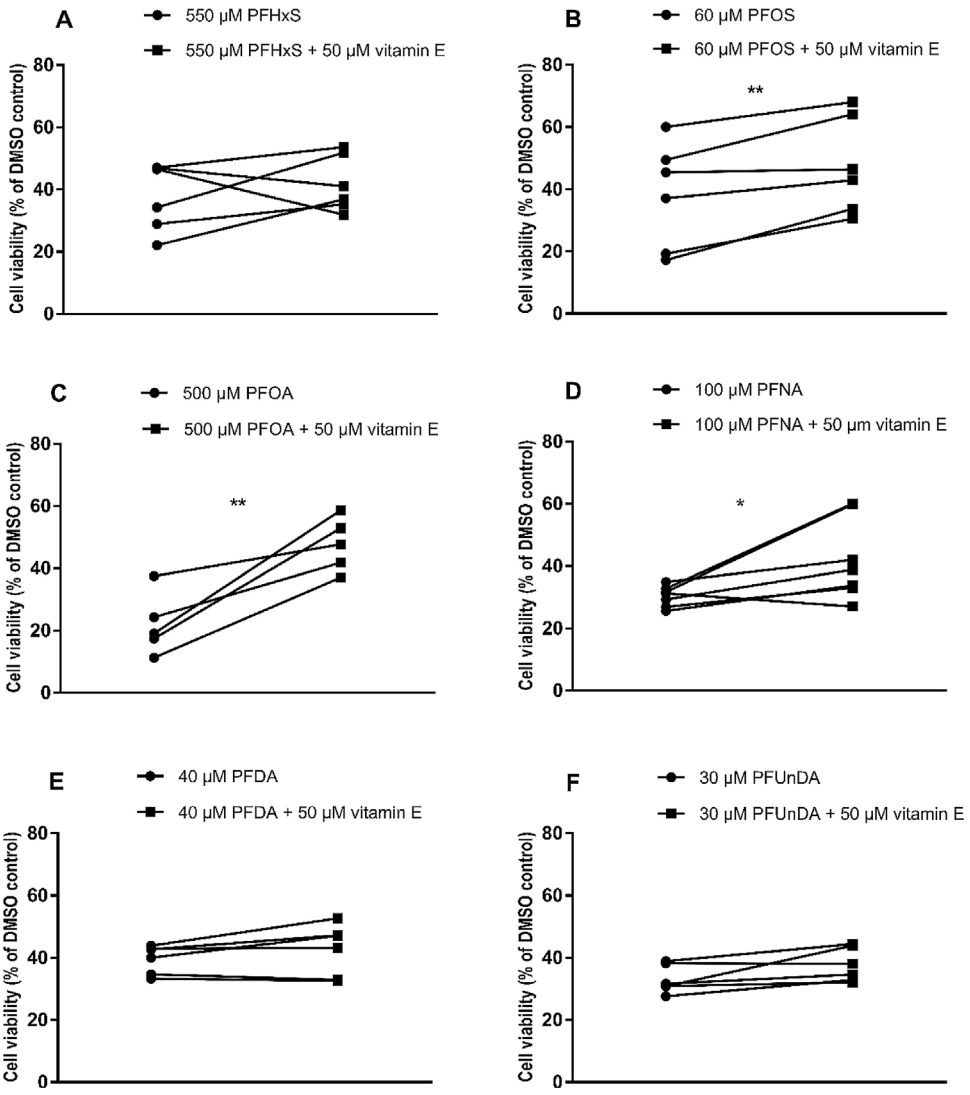

Fig. 5. Neuroprotective effect of vitamin E on PFAA-induced cytotoxicity.
Viability was assessed with the MTT assay after 24 h exposure of CGNs to A) 550 µM PFHxS, B) 60 µM PFOS, C) 500 µM PFOA, D) 100 µM PFNA, E) 40 µM PFDA and F) 30 µM PFUnDA alone and in conjunction with 50 µM of the antioxidant vitamin E. All values are relative to the 0.1% DMSO control in each experiment (defined as 100%). A two-tailed paired *t*-test was used to assess statistical differences in viability between CGNs treated with each PFAA only as compared to the PFAA in conjunction with vitamin E. The paired measurements with and without vitamin E from each individual experiment are displayed and linked by an interconnecting line (n = 5–7 independent experiments, each from a separate cell isolation, with each condition performed in triplicate)

2.8. Statistical analysis

Statistical analyses and calculations were carried out using GraphPad Prism 5 (GraphPad Software, San Diego, CA, USA) and IBM SPSS Statistics, Version 23.0 (IBM Corp., Armonk, NY, USA). Prior to statistical testing, homogeneity of variances between group means was tested with a Brown-Forsythe test. For multiple pairwise comparisons between groups, in the case of homoscedasticity, a one-way ANOVA was performed, followed by a Dunnett's post hoc test for comparison of each group mean with the DMSO control. Where heteroscedasticity was detected, a Welch's ANOVA followed by a Games-Howell post hoc test was used. For the time-dependent cytotoxicity studies, a two-way ANOVA was used to assess the effects of time and exposure on cell viability, and a Dunnett's post hoc test was conducted to assess differences between exposed cells and the 0.1% DMSO control at each time-point. For the assessment of significant increases in viability in CGNs treated with the different PFAAs and vitamin E as compared to PFAA treatment only, a two-tailed paired *t*-test was used. In all the experiments conducted, a *p*-value of < 0.05 was regarded as statistically significant. Best fit concentration-response curves for cell-viability and estimation of LC_{50} values after exposure to PFAAs were obtained by non-linear regression in Prism 5, after log transformation of concentrations, with a variable slope model, and top and bottom values constrained to 100 and 0%. For the lipid peroxidation rates, data obtained by linear regression in Prism 5 (slopes of the curves) were transformed into daily %-values of the respective DMSO controls (with or without cumOOH) set to 100%, allowing pooling of normalised data from different days followed by an ANOVA and a Dunnett's post hoc test.

3. Results

3.1. Concentration-response curves and LC_{50} values for PFAA-induced cytotoxicity

For the assessment of cytotoxicity after PFAA exposure CGNs were exposed to increasing concentrations of the six PFAAs for 24 h

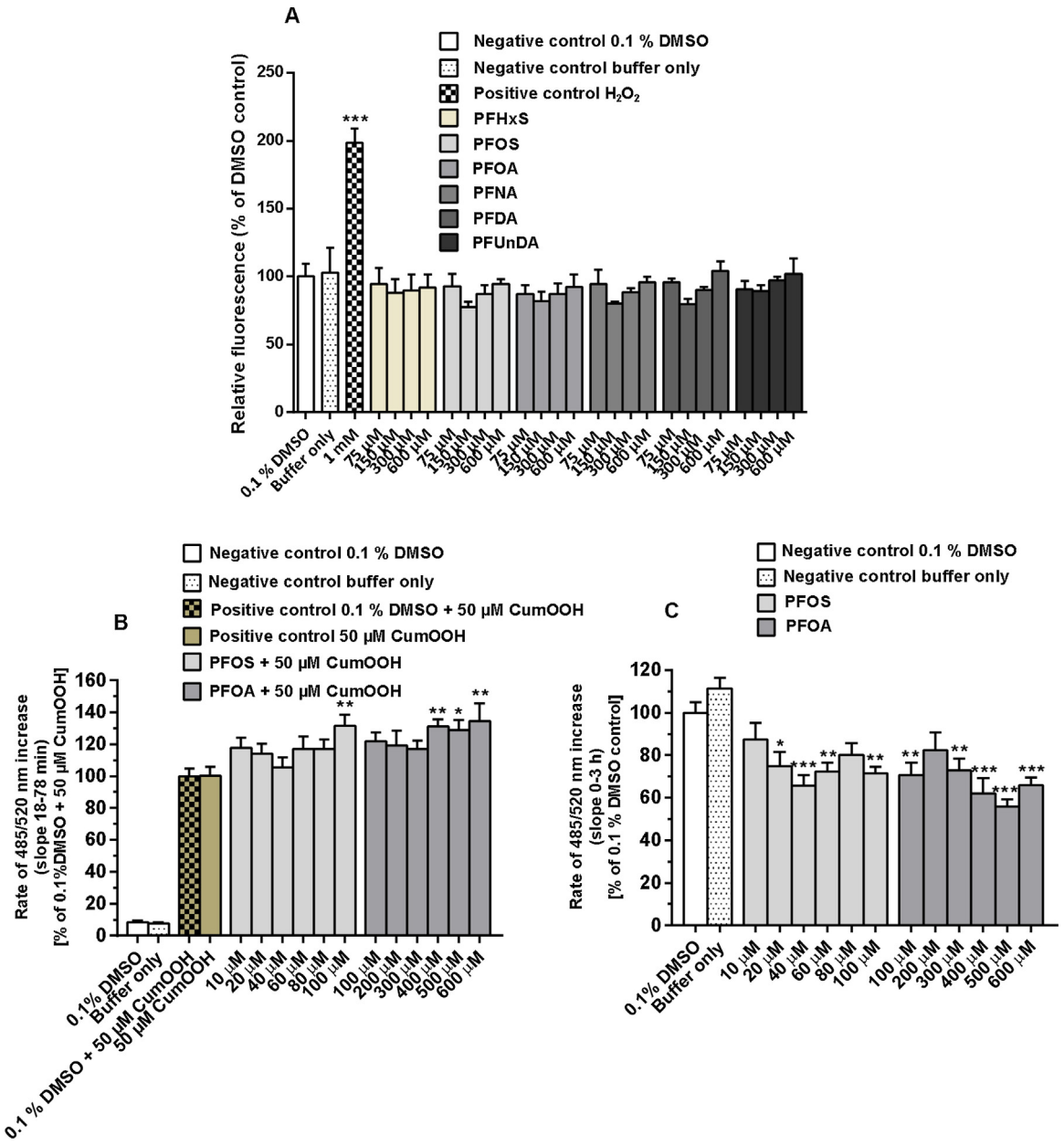

Fig. 6. Assessment of ROS production and lipid-peroxidation after PFAA exposure.
A) ROS production, expressed as relative fluorescence, was assessed during 3 h exposure of CGNs to increasing concentrations of PFHxS, PFOS, PFOA, PFNA, PFDA and PFUnDA, using the DCF-assay. H_2O_2 (1 mM) was included as a positive control. All values were calculated as area under the curve (AUC) relative to the 0.1% DMSO control (defined as 100%). Mean values + SEM are displayed. B) Lipid peroxidation was assessed during 1 h 30 min using the probe C_{11}-BODIPY, after co-treatment of cells with 50 µM cumOOH and increasing concentrations of PFOS and PFOA. The slopes for the increase in green fluorescence (reflecting rate of lipid peroxidation) for each exposure were determined by linear regression and expressed as % of the slope for 0.1% DMSO + 50 µM cumOOH. Mean values + SEM are displayed. C) Lipid peroxidation was assessed during 3 h using the probe C11-BODIPY, after exposure to increasing concentrations of PFOS and PFOA. The slopes are expressed as % of the slope for the 0.1% DMSO control. Mean values + SEM are displayed. Statistical differences for A, B and C graph data were assessed with a one-way ANOVA and a Dunnett's post hoc test (n = 3 independent experiments, each from a separate cell isolation, with each condition tested in triplicate). *,**,*** indicate significant differences ($p < 0.05$, $p < 0.01$ and $p < 0.001$) relative to the respective controls (0.1% DMSO in A and C, and 0.1% DMSO + cumOOH for B)

and cell viability estimated using the MTT and trypan blue assays. PFAA exposure significantly affected cell viability for all the PFAAs as measured with both assays (see Supplementary table S1 for statistical results).

The concentration-response curves for the individual PFAAs obtained with the two assays and values significantly different from the 0.1% DMSO control are presented in Fig. 3. Significant reductions in cell viability as compared to the 0.1% DMSO control were induced at concentrations at (equal to the lowest observed effect concentration (LOEC))/or above 400 and 450 µM PFHxS, 20 and 60 µM PFOS, 300 and 400 µM PFOA, 40 and 80 µM PFNA, 20 and 30 µM PFDA and 15 and 40 µM PFUnDA with the MTT and trypan blue assays, respectively.

LC_{50} values for the six PFAAs were comparable for the two methods, whereas the LOECs and the no observed effect concentrations (NOECs) deviated somewhat more (Table 2). For the MTT and trypan blue assays the potencies of the six PFAAs, as observed by the LC_{50} values, were in descending order: PFUnDA

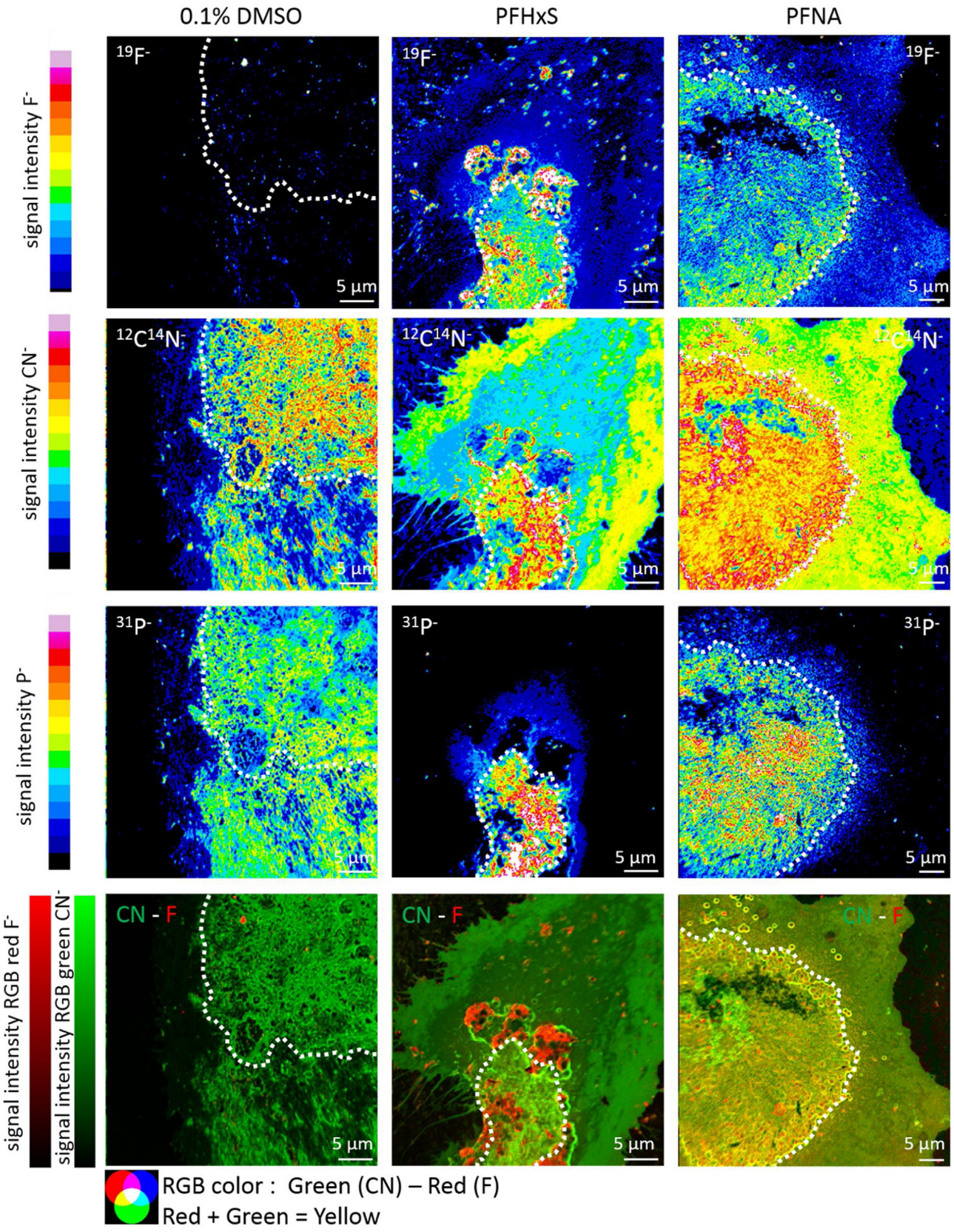

Fig. 7. Distribution of PFAAs on the CGN-membrane of a single cell.
Elemental distribution of $^{19}F^-$ (first row) $^{12}C^{14}N^-$ (second row) $^{31}P^-$ (third row) and the overlay of $^{19}F^-$ on $^{12}C^{14}N^-$(fourth row) on the surface of single cerebellar granule neurons is shown in Fig. 7. The signals were simultaneously collected with independent electron multipliers. Fluorine images visualize the localization of the perfluorinated compounds. Ubiquitous carbon and nitrogen atoms that recombine to CN-ions provide pictures of the cell morphology similar to those obtained with optical microscopy (signal assimilated to the proteins). The phosphorus images allow to localize the membrane and the genetic information (phospholipids, DNA, nucleus). For clarity the outline of the nucleus is indicated by the white dotted line. Cells were exposed for 24 h to 0.1% DMSO (control) left column, or 10 μM of the respective compounds. The middle and

> PFDA > PFOS > PFNA > PFOA > PFHxS and PFUnDA = PFDA > PFOS > PFNA > PFOA > PFHxS, respectively.

3.2. Time-dependent effects on cell viability after PFAA exposure

Time-dependent effects on cell viability were assessed using the MTT-assay after exposure of CGNs to a single concentration of the six PFAAs for different time-points. A concentration of each compound producing equipotent effects at 24 h was used (see Section 2.5.2). The time-curves for all the six PFAAs are compared in Fig. 4. Values are expressed as percentage of the 0.1% DMSO control at each time-point (defined as 100%). There was significant interaction between the effects of time and exposure on cell viability ($F_{54,171} = 5.95$, $p < 0.001$). Simple main effect analysis showed that both time ($F_{9,171} = 28.12$, $p < 0.001$) and exposure ($F_{6,171} = 202.1$, $p < 0.001$) had significant effects on cell viability. For the two PFSAs, there was a clear difference in the onset of effects on viability (Fig. 4). PFOS induced significant effects on viability within the first 60 min of exposure, with reductions of 28, 46 and 62% at 10, 30 and 60 min, respectively ($p < 0.001$ for all). Thereafter cell viability remained constant for the rest of the exposure period. For PFHxS on the other hand, a significant decrease in cell viability was only observed after 24 h of exposure, with a reduction of 48% ($p < 0.001$). For the PFCAs also two distinct patterns appeared. Whereas PFDA and PFUnDA induced maximum effect already after 30 min of exposure, with reductions in cell viability of 40 and 29% ($p < 0.01$ and $p < 0.001$) at 10 min and 55 and 53% at 30 min ($p < 0.001$ for both), respectively, PFOA and PFNA significantly reduced viability from 12 h onwards. The reductions in viability were 35 and 39% at 12 h, 85 and 46% at 18 h and 88 and 52% at 24 h, respectively ($p < 0.001$ for all). PFNA exposure also resulted in around 20% reduction in cell-viability at the earlier time points, but only at 60 min of exposure, the reduction was statistically significant ($p < 0.05$).

3.3. Effects of vitamin E on PFAA-induced cytotoxicity

To get an indication on the involvement of cell membrane related oxidative stress in the PFAA-induced cytotoxicity, CGNs were co-incubated with the six PFAAs and 50 μM of the lipophilic antioxidant vitamin E for 24 h. Results of the assay are presented in Fig. 5. The largest protective effect of vitamin E was seen for the PFOA-induced cytotoxicity, where cell death was reduced with 26% ($p < 0.01$). Also for PFNA and PFOS, small statistically significant reductions in cell death of 12 and 10% were observed ($p < 0.05$ and $p < 0.01$, respectively). No significant protective effect of vitamin E was detected for PFHxS, PFDA or PFUnDA.

3.4. Assessment of PFAA-induced ROS production

Intracellular CGN ROS production (DCF assay) after exposure to increasing concentrations of PFAAs for 3 h, is shown in Fig. 6A. There was no significant increase in ROS production in cells treated with any of the PFAAs at the concentrations used, whereas the positive control H_2O_2 increased ROS production with 99% as compared to the 0.1% DMSO control, ANOVA ($F_{26,54} = 7.08$, $p < 0.001$), with a Dunnett's post hoc test ($p < 0.001$).

3.5. Lipid peroxidation after exposure to PFOA and PFOS

For experiments conducted with the inducer cumOOH, a significant increase in the rate of lipid peroxidation was detected after PFOS and PFOA exposure (ANOVA ($F_{15,46} = 45.28$, $p < 0.001$)) (Fig. 6B). The increases were 32% after exposure to 100 μM PFOS ($p < 0.01$) and 29–34% after exposure to 400–600 μM PFOA ($p < 0.05$), Dunnett's post hoc test. For the experiments conducted without inducer, no increase in the rate of lipid peroxidation was observed, however a significant decrease in lipid peroxidation rate was observed for PFOS and PFOA at all tested concentrations except 10 and 80 μM PFOS and 200 μM PFOA (ANOVA ($F_{13,122} = 7.81$, $p < 0.001$)) (Fig. 6C).

3.6. Distribution of PFAAs on the nerve cell membrane, visualised using NanoSIMS imaging

PFOS, PFHxS and PFUnDA accumulated very distinctly in the cell membrane with large hotspots. PFOA, PFDA and PFNA accumulated in a more diffuse manner with much smaller hotspots when compared to the first group of chemicals. A representative image of one cell per exposure have been displayed for the DMSO control, PFHxS and PFNA in Fig. 7, as examples of the different distribution patterns. In order to compare the intensities of the SIMS signals, for each element (ion) detected, the images are represented with the same intensity scale. Images for PFOS, PFOA, PFDA and PFUnDA are included under the Supplementary material section. In DMSO treated cells, a very low signal for fluorine was observed. Limits of detection in the NanoSIMS50 are dependent on the element in question and in general halogens, and here again fluorine, has the best detection limit of all elements. Some traces of fluorine are therefore always observed. However, in all treated cells fluorine signals could not only be detected providing information on the localization of the perfluorinated compounds, but were also much stronger than in the controls.

4. Discussion

In the present study, we found that the overall cytotoxicity evoked in CGNs by some of the most prominent PFAAs detected in human blood and brains of wildlife, as well as the onset of reduction in viability, is related to toxicant carbon chain length and functional group attached. Vitamin E had a small, but statistically significant protective effect against reductions in cell viability for three of the PFAAs; PFOS, PFOA and PFNA. No ROS production was detected in the present study for any of the six PFAAs. However, PFOA and PFOS significantly accelerated the rate of lipid peroxidation in CGNs after co-exposure with the inducer cumOOH. There was a clear difference in the way the different PFAAs accumulated in the cell membrane. Whereas PFHxS, PFOS and PFUnDA accumulated in an aggregated manner, PFOA, PFNA and PFDA showed a more dispersed pattern of distribution.

In the present study, we used two different assays for the assessment of cell viability, as these detect different end-points. The MTT assay is a rapid, non-subjective, colorimetric assay, used for the assessment of mitochondrial metabolic activity as a measure of cell viability. The trypan blue assay, assessing cell membrane damage, is a more subjective and time-consuming assay, where the detection of dead and live cells is dependent on the individual evaluation of the investigator. The MTT assay

right columns show the distribution pattern on cells exposed to PFHxS and PFNA, respectively. Images for PFOS, PFOA, PFDA and PFUnDA may be found under the Supplementary material. Scale bar is 5 μm. The colour scale for the signal intensity of the F, CN and P-images runs from black to white, with white colours reflecting the highest intensity. For each individual ion detected the intensity scale is common (i.e. from 1 to 400 Cts/s for F^- as compared with the scale 100–10 000 for CN^- ions and 1–1000 for P^-). The colour scale for the green and red signal intensity for the combined CN-F images is also shown, as well as an illustration on how the overlay of red and green colours is resulting in a yellow tone (RGB mode)

however, has been criticised for possibly resulting in false positive or negative results. However, as the cells in the CGN-cultures are post-mitotic, the problems with cells dividing at different rates in different plates/wells is not causing a problem as may be experienced for the MTT assay with cell-lines or other cells in division.

After obtaining comparable concentration-response curves (Fig. 3) and LC_{50} values (Table 2) for the six different PFAAs using the two assays, we concluded that the MTT assay was suitable for further studies on cell viability in CGNs after PFAA exposure. Although the curves for the two assays were comparable, some variability was observed. For PFOS, the concentration-response curve obtained using MTT was shifted to the left as compared to when using the trypan blue assay, and lower NOEC, LOEC and LC_{50} values were detected. Also for PFUnDA, the values were lower for the MTT assay. For the rest of the PFAAs the curves deviated less. Here, the higher NOEC and LOEC values observed with the trypan blue assay may to some extent have been influenced by the low number of experiments performed, and fewer concentrations included, for this assay.

As illustrated in Table 2 by the LC_{50} values presented, toxicity increased with increasing carbon chain length for both the sulfonated and carboxylated PFAAs. PFHxS, the shortest PFSA, was clearly much less toxic than PFOS, which has two more fluorinated carbon atoms in the chain. Also PFOA, was much less toxic than its longer chained PFCA equivalents PFNA, PFDA and PFUnDA. Interestingly, PFDA and PFUnDA were even more potent inducers of cytotoxicity, than PFOS. Recently published studies in the brain from polar bears show that although the concentrations of PFOS has decreased over the last decade, concentrations of the longer chained PFCAs, including PFUnDA are increasing (Eggers Pedersen et al., 2015; Greaves et al., 2013). This is likely to reflect current industrial uses of PFAAs, a phase out of PFOS, and could as suggested by Eggers Pedersen et al. (2015), be a result of a shift from the use of the PFOS precursor PFOSF in products towards use of fluorotelomers, potential PFCA precursors.

In the present study the concentrations used for the PFAAs studied were selected to be able to construct full concentration-response curves for the various compounds, and to compare potential toxicity after 24 h exposure. The concentrations used and found to induce toxicity are much higher than serum levels found in the general population. The latter typically ranging from 0.4 for the least prominent compounds to 40 ng/ml for PFOS the most prominent (Calafat et al., 2007; Haug et al., 2010b; Karrman et al., 2007). The concentrations used in our study are thus most likely to be relevant in occupational settings where high levels of perfluorinated compounds may be measured. Several studies in occupationally exposed workers in fluorochemical plants report levels of PFHxS, PFOA and PFOS, whereas no such studies on levels of PFNA, PFDA or PFUnDA were found. In a recent study by Fu et al. (2016), high serum levels of PFHxS, PFOA and PFOS, were detected. The median and maximum reported concentrations were 764 ng/ml and 19837 ng/ml for PFHxS (corresponding to 2 and 50 μM) 427 ng/ml and 32000 ng/ml for PFOA (corresponding to 1 and 77 μM) and 1725 and 118000 ng/ml for PFOS (corresponding to 3 and 236 μM).

Serum levels of the investigated compounds have been widely reported for the general population (Calafat et al., 2007; Haug et al., 2010b; Karrman et al., 2007). However, as far as the authors are aware only one study by Maestri et al. (2006) report levels of PFOS and PFOA in the human brain. Levels of the two compounds in the brain corresponded to 25 and 17% of the levels in serum, respectively. This is line with what has been measured in other mammals. In the study by Ahrens et al. (2009) in harbour seals levels of PFOS and PFOA corresponded to 28 and 10% of serum levels. In a study by Greaves et al. (2012) in polar bears concentrations were 28 and 8% of serum. The brain levels of PFHxS, PFNA, PFDA, PFUnDA, PFDoDA, PFTriDA and perfluorotetradecanoic acid (PFTeDA), were also measured in the two studies. In harbour seals the values for the various compounds were 50, 31, 35, 62, 109, 96 and 125% of serum levels, respectively. In the polar bears they were 8, 11, 30, 73, 140, 220 and 280% of serum levels. Concentrations of perfluoropentadecanoic acid (PFPeDA), also measured in polar bears, were 770% of the levels in serum. This indicates an increased accumulation in the brain with increasing carbon chain length for the PFCAs.

Examining the results obtained in the present study in light of these percentages, it is clear that the LC_{50} values determined for PFHxS and PFOA are higher than concentrations reached in serum (5–10x), and thus also the brain, of occupationally exposed workers. For PFOS however, assuming a concentration in the brain as 25% of the level in serum, the highest values reported for the occupationally exposed workers above would correspond to a brain level of 60 μM. This is higher than the NOEC values reported for PFOS with both assays in the present study, and also higher than the LC_{50} value obtained with the MTT assay/just below the LC_{50} value for the trypan blue assay (Table 2). As discussed by Mariussen (2012) it is also conceivable that PFOS at higher exposure concentrations accumulates in the brain to a greater extent than at lower exposure concentrations. This, possibly due to a saturation kinetic in the liver, with more PFOS being available to reach the brain at higher concentrations. No industrial studies from fluorochemical plants could be found for the longer chained PFCAs. However, due to the higher cellular toxicity observed with increasing carbon chain length in the present study, their apparent increased accumulation in brain vs. serum, as well as their reported environmental increase, future studies with the longer chained PFCAs (C_{10}–C_{15}) are warranted.

In regards to the study of effects of functional group and similar carbon chain length, some studies compare PFOS with PFOA (e.g. Hagenaars et al. (2011) and Gorrochategui et al. (2014)), whereas other studies compare it to PFNA (e.g. Nobels et al. (2010)). PFOS and PFOA have the same total number of carbon atoms in the molecule (including the functional groups), whereas PFOS and PFNA have the same total number of fluorinated carbon atoms in the chain. From the results of our study, it is clear that in CGNs treated with PFAAs with the same total number of carbon atoms in the chain, toxicity was markedly increased when the perfluorinated carbon chain was attached to a sulfonate group as compared to a carboxyl group (PFOS vs PFOA). When comparing molecules with the same number of fluorinated carbon atoms in the chain (PFOS vs PFNA), the difference in toxicity was less pronounced (Table 2).

There was a clear difference in the onset of reductions in viability in CGNs exposed to concentrations of the six PFAAs giving equipotent effects at 24 h (Fig. 4). The three most toxic compounds; PFOS, the longer chained PFSA as well as PFDA and PFUnDA, the two longest PFCAs, rapidly reduced viability within one hour of exposure, which thereafter remained constant for the rest of the exposure period. Even after only 10 min, significant reductions in viability were observed. PFOA and PFNA, the two shortest PFCAs, as well as PFHxS, the shortest PFSA, showed a completely different pattern of toxicity, with a slow induction, and decreases in cell viability starting somewhere between 6 h and 12 h of exposure. The reductions in cell viability being significant only after 12 h for PFOA and PFNA, and at 24 h for PFHxS. The early small, but statistically insignificant decrease in viability observed for PFNA at the time-points prior to 12 h, could possibly reflect the death of an especially sensitive subpopulation of CGNs. Studies in CGN cultures exposed to glutamate have previously shown that certain sensitive subpopulations of neurons may die by early necrosis, followed by delayed apoptosis in recovering cells. A distinction

between cell death induced by necrosis or apoptosis is not straight forward, and cells showing both kinds of features may co-exist in culture (Ankarcrona et al., 1995). The aim of the present study was not to determine the mechanism of cell death induction, but based on the results showed herein, experiments addressing this represent interesting future studies.

What may be the cause of the difference in onset of reductions in viability is not clear, but one possibility could be differential uptake of compounds by the cells as well as variable effects on membrane permeability. Previous studies in JEG-3 cells using equimolar concentrations (6 μM) of PFAAs have shown that PFOS as well as the longer chained PFDoDA were detected at much higher levels intracellularly right after dosing than PFOA and PFNA. They also reached much higher maximum levels after 5 h of exposure (Gorrochategui et al., 2014). In the same study PFHxS, did not induce significant toxicity nor did it reach measurable intracellular levels. PFAAs are assumed to incorporate into the cell membrane, and Kleszczynski et al. (2007) hypothesised that fluorocarbons with a longer aliphatic chain would incorporate into biological membranes in a more organised manner resulting in disruption of structure, possibly competing with physiological fatty acids. PFOS has also been found capable of altering membrane permeability as well as membrane fluidity (at 33 and 100 μM) in fish leucocytes (Hu et al., 2003). In the mentioned study, the action of PFOS on the cell membrane was rapid, and the authors stated that the short time until the onset of observed effects, in addition to the short chain length of PFOS, would preclude its incorporation into membrane lipids. In the present study, we observed two distinct patterns of accumulation for the PFAAs studied. PFHxS and PFOS, the two PFSAs as well as PFUnDA, the longer chained PFCA, accumulated in an aggregated manner. The accumulation of PFOS in highly specific areas of the membrane has been reported before (Gutleb et al., 2012). This fact also contradicts the assumption of a homogenous partition of PFOS into lipid bilayers based on the chemical structure that resembles fatty acids. Hu et al. (2003) hypothesised that PFOS was more likely to be active at lipid/protein interfaces within the membrane. The NanoSIMS technique applied in the present study was only used to detect elements on the surface of the cell. To minimise the destruction of the surface of the membrane, we chose analytical conditions without the implantation of Cesium (Cs), as described in Kraft et al. (2006) and Audinot et al. (2011), as Cs implantation would result in sputtering of around 15–20 nm of the sample. The NanoSIMS technique may also be adapted to study intracellular distribution of elements. This would however require cell sectioning preceded by embedding of cells in resins. Unfortunately, current available resins contain fluorine-based chemicals, leading to a high F-isotope background, thus precluding the visualisation of PFAS-based chemicals. Based on the present study it is therefore not possible to conclude on the uptake and intracellular accumulation of the investigated compounds, which will be dependent on the emergence of non-fluorine-based resins. PFAAs with different chain lengths have been hypothesised to have variable lipid solubility as well as affinity to different proteins (Greaves et al., 2012), which may perhaps to some extent explain variations in the cell membrane distribution pattern. One may speculate that the aggregated accumulation observed for some of the compounds could be due to preferential interaction with proteins, only found at specific areas of the cell membrane. This is however not possible to conclude from the present experiment.

A reduction in cell death at 24 h after exposure to PFOS, PFOA and PFNA in conjunction with the fast acting, lipid soluble antioxidant vitamin E, which has got lipid peroxyl radical-scavenging properties (Jiang, 2014), indicated that oxidative stress may be involved in the cytotoxicity. The highest protective effect after co-treatment with vitamin E was observed for PFOA, whereas for PFOS and PFNA the reductions in cell death were rather small. Interestingly, no ROS production was observed with the DCF assay in CGNs exposed to increasing concentrations of the six different PFAAs for 3 h (Fig. 6A). This is in contrast to the studies by Lee et al. (2012) and Reistad et al. (2013) where increases in ROS production were observed with the same assay and cell type after exposure to 3 and 30 μM and 25, 50 and 100 μM PFOS, respectively. In the study by Reistad et al. (2013) PFOA did also cause significant induction of ROS production at concentrations of 12, 25, 50 and 100 μM. The lack of concordance between our studies could possibly be explained by methodological differences as well as differences in the sensitivity of equipment used for measurements, or differences in sensitivity between cultures.

In the study by Reistad et al. (2013) cells were exposed to the toxicants in 5 cm dishes before they were loosened from the plate and transferred to 96 well plates for assessment of ROS production. In the present study cells were grown directly in 96 well plates before exposure to toxicants and assessment of ROS production. One may assume that cells being detached from the plate having their interconnecting neuronal network disrupted, could be experiencing a higher state of cellular stress than cells exposed with their neuronal network intact. This could perhaps explain some of the differences in the results between our studies. In the study by Lee et al. (2012) cells were, as in the present study, seeded directly in 96-well plates, but were analysed by live image fluorescence microscopy.

Also in our lipid peroxidation studies with PFOS and PFOA, an increase in lipid peroxidation was only observed after co-treatment with another stressor, the lipid peroxidation-inducer cumOOH (Fig. 6B), whereas no increase in lipid peroxidation was observed when cells were exposed without inducer (Fig. 6C). In the time-course studies PFOS induced most of its effects on viability within 60 min exposure. As lipid peroxidation without inducer was measured for 3 h, our studies therefore indicate that lipid peroxidation is not a main initiator of PFOS-induced death in CGNs. In the time-course studies with PFOA on the other hand cell viability was only significantly affected after 12 h exposure. ROS production and lipid peroxidation were only measured for 3 h. A delayed onset of toxicity may thus potentially explain why there was an absence of ROS production and lipid peroxidation in PFOA treated cells at 3 h, at the same time as vitamin E significantly protected against cytotoxicity after 24 h exposure. When cells were exposed to the lipid peroxidation inducer cumOOH in conjunction with the PFAAs, the highest concentration of PFOS as well as the three highest concentrations of PFOA significantly accelerated the induced lipid-peroxidation. This could perhaps indicate that these compounds at high concentrations have the capability to worsen inflammation-induced lipid peroxidation. As we overall used a higher concentration of PFOA than PFOS in the lipid peroxidation studies, of the two, PFOS was a more potent accelerator of lipid peroxidation.

A significant decrease in the measured lipid-peroxidation was observed for both compounds at most of the tested concentrations, in the experiments conducted without inducer (Fig. 6C). Whether this is a result of an upregulation of antioxidant defence systems in the exposed cells as compared to the DMSO control, resulting in measurements of lipid-peroxidation markers that are lower than in the control, could be speculated, but would need further confirmation. In a study by Chen et al. (2014) in SH-SY5Y cells, exposure to 25 and 50 μM PFOS caused a significant increase in the activity of superoxide dismutase (SOD).

5. Conclusion

In conclusion, the cytotoxicity induced by long chained PFAAs in CGNs increases with elongation of the carbon chain. For

compounds of similar chain length attached to different functional groups, possession of a sulfonate group increased the toxicity as compared to attachment to a carboxyl group. The timing of PFAA-induced effects on viability followed two distinct patterns. Whereas PFOS and the longer chained PFUnDA and PFDA rapidly reduced viability, effects on viability after exposure to PFHxS, PFOA and PFNA occurred at a much slower rate. The observed pattern of PFAA-accumulation on the nerve cell membrane was variable. The sulfonated PFHxS and PFOS as well as PFUnDA, the longest chained PFCA, accumulated in an aggregated form, whereas PFOA, PFNA and PFDA showed a more dispersed distribution. PFOS and PFOA accelerated cumOOH-induced lipid peroxidation in CGNs.

Conflict of interest statement

The authors declare that there are no conflicts of interest

Acknowledgement

This study was funded by the Research Council of Norway [grant numbers 204361/H10, 213076/H10].

Appendix A. Supplementary data

Supplementary data associated with this article can be found, in the online version, at http://dx.doi.org/10.1016/j.neuro.2017.09.005.

References

Ahrens, L., Siebert, U., Ebinghaus, R., 2009. Total body burden and tissue distribution of polyfluorinated compounds in harbor seals (Phoca vitulina) from the German Bight. Mar. Pollut. Bull. 58 (4), 520–525.
Ankarcrona, M., Dypbukt, J.M., Bonfoco, E., Zhivotovsky, B., Orrenius, S., Lipton, S.A., Nicotera, P., 1995. Glutamate-induced neuronal death: a succession of necrosis or apoptosis depending on mitochondrial function. Neuron 15 (4), 961–973.
Audinot, J.N., Cabin-Flaman, A., Philipp, P., Legent, G., Wirtz, T., Migeon, H.N., 2011. NanoSIMS50 imaging of thin samples coupled with neutral cesium deposition. Surf. Interface Anal. 43 (1–2), 302–305.
Audinot, J.N., Georgantzopoulou, A., Piret, J.P., Gutleb, A.C., Dowsett, D., Migeon, H. N., Hoffmann, L., 2013. Identification and localization of nanoparticles in tissues by mass spectrometry. Surf. Interface Anal. 45 (1), 230–233.
Ayala, A., Munoz, M.F., Arguelles, S., 2014. Lipid peroxidation: production, metabolism, and signaling mechanisms of malondialdehyde and 4-hydroxy-2-nonenal. Oxid. Med. Cell. Longev. 2014, 360438.
Berntsen, H.F., Wigestrand, M.B., Bogen, I.L., Fonnum, F., Walaas, S.I., Moldes-Anaya, A., 2013. Mechanisms of penitrem-induced cerebellar granule neuron death in vitro: possible involvement of GABAA receptors and oxidative processes. Neurotoxicology 35, 129–136.
Buck, R.C., Franklin, J., Berger, U., Conder, J.M., Cousins, I.T., de Voogt, P., Jensen, A.A., Kannan, K., Mabury, S.A., van Leeuwen, S.P., 2011. Perfluoroalkyl and polyfluoroalkyl substances in the environment: terminology, classification, and origins. Integr. Environ. Assess. Manag. 7 (4), 513–541.
Calafat, A.M., Wong, L.Y., Kuklenyik, Z., Reidy, J.A., Needham, L.L., 2007. Polyfluoroalkyl chemicals in the U.S. population: data from the national health and nutrition examination survey (NHANES) 2003–2004 and comparisons with NHANES 1999–2000. Environ. Health Perspect. 115 (11), 1596–1602.
Chen, N., Li, J., Li, D., Yang, Y., He, D., 2014. Chronic exposure to perfluorooctane sulfonate induces behavior defects and neurotoxicity through oxidative damages, in vivo and in vitro. PLoS One 9 (11), e113453.
Drejer, J., Larsson, O.M., Schousboe, A., 1982. Characterization of L-glutamate uptake into and release from astrocytes and neurons cultured from different brain regions. Exp. Brain Res. 47 (2), 259–269.
Eggers Pedersen, K., Basu, N., Letcher, R., Greaves, A.K., Sonne, C., Dietz, R., Styrishave, B., 2015. Brain region-specific perfluoroalkylated sulfonate (PFSA) and carboxylic acid (PFCA) accumulation and neurochemical biomarker responses in east Greenland polar bears (Ursus maritimus). Environ. Res. 138, 22–31.
Fu, J., Gao, Y., Cui, L., Wang, T., Liang, Y., Qu, G., Yuan, B., Wang, Y., Zhang, A., Jiang, G., 2016. Occurrence, temporal trends, and half-lives of perfluoroalkyl acids (PFAAs) in occupational workers in China. Sci. Rep. 6, 38039.
Gallo, V., Ciotti, M.T., Coletti, A., Aloisi, F., Levi, G., 1982. Selective release of glutamate from cerebellar granule cells differentiating in culture. Proc. Natl. Acad. Sci. U. S. A. 79 (24), 7919–7923.
Georgantzopoulou, A., Balachandran, Y.L., Rosenkranz, P., Dusinska, M., Lankoff, A., Wojewodzka, M., Kruszewski, M., Guignard, C., Audinot, J.N., Girija, S., Hoffmann, L., Gutleb, A.C., 2013. Ag nanoparticles: size- and surface-dependent effects on model aquatic organisms and uptake evaluation with NanoSIMS. Nanotoxicology 7 (7), 1168–1178.
Giesy, J.P., Kannan, K., 2001. Global distribution of perfluorooctane sulfonate in wildlife. Environ. Sci. Technol. 35 (7), 1339–1342.
Gorrochategui, E., Perez-Albaladejo, E., Casas, J., Lacorte, S., Porte, C., 2014. Perfluorinated chemicals: differential toxicity, inhibition of aromatase activity and alteration of cellular lipids in human placental cells. Toxicol. Appl. Pharmacol. 277 (2), 124–130.
Greaves, A.K., Letcher, R.J., Sonne, C., Dietz, R., Born, E.W., 2012. Tissue-specific concentrations and patterns of perfluoroalkyl carboxylates and sulfonates in East Greenland polar bears. Environ. Sci. Technol. 46 (21), 11575–11583.
Greaves, A.K., Letcher, R.J., Sonne, C., Dietz, R., 2013. Brain region distribution and patterns of bioaccumulative perfluoroalkyl carboxylates and sulfonates in east greenland polar bears (Ursus maritimus). Environ. Toxicol. Chem. 32 (3), 713–722.
Gutleb, A.C., Freitas, J., Murk, A.J., Verhaegen, S., Ropstad, E., Udelhoven, T., Hoffmann, L., Audinot, J.N., 2012. NanoSIMS50 – a powerful tool to elucidate cellular localization of halogenated organic compounds. Anal. Bioanal. Chem. 404 (9), 2693–2698.
Hagenaars, A., Vergauwen, L., De Coen, W., Knapen, D., 2011. Structure-activity relationship assessment of four perfluorinated chemicals using a prolonged zebrafish early life stage test. Chemosphere 82 (5), 764–772.
Halliwell, B., 1997. Antioxidants and human disease: a general introduction. Nutr. Rev. 55 (1 Pt 2), S44–S49 (discussion S49-52).
Halsne, R., Tandberg, J.I., Lobert, V.H., Ostby, G.C., Thoen, E., Ropstad, E., Verhaegen, S., 2016. Effects of perfluorinated alkyl acids on cellular responses of MCF-10A mammary epithelial cells in monolayers and on acini formation in vitro. Toxicol. Lett. 259, 95–107.
Hansen, K.J., Clemen, L.A., Ellefson, M.E., Johnson, H.O., 2001. Compound-specific, quantitative characterization of organic fluorochemicals in biological matrices. Environ. Sci. Technol. 35 (4), 766–770.
Haug, L.S., Salihovic, S., Jogsten, I.E., Thomsen, C., van Bavel, B., Lindstrom, G., Becher, G., 2010a. Levels in food and beverages and daily intake of perfluorinated compounds in Norway. Chemosphere 80 (10), 1137–1143.
Haug, L.S., Thomsen, C., Brantsaeter, A.L., Kvalem, H.E., Haugen, M., Becher, G., Alexander, J., Meltzer, H.M., Knutsen, H.K., 2010b. Diet and particularly seafood are major sources of perfluorinated compounds in humans. Environ. Int. 36 (7), 772–778.
Hofer, T., Jorgensen, T.O., Olsen, R.L., 2014. Comparison of food antioxidants and iron chelators in two cellular free radical assays: strong protection by luteolin. J. Agric. Food Chem. 62 (33), 8402–8410.
Hofer, T., 2001. Oxidation of 2′-deoxyguanosine by H 2 O 2–ascorbate: evidence against free OH and thermodynamic support for two-electron reduction of H 2 O 2. J. Chem. Soc. Perkin Trans. 2 (2), 210–213.
Holzer, J., Goen, T., Rauchfuss, K., Kraft, M., Angerer, J., Kleeschulte, P., Wilhelm, M., 2009. One-year follow-up of perfluorinated compounds in plasma of German residents from Arnsberg formerly exposed to PFOA-contaminated drinking water. Int. J. Hyg. Environ. Health 212 (5), 499–504.
Hoyer, B.B., Ramlau-Hansen, C.H., Obel, C., Pedersen, H.S., Hernik, A., Ogniev, V., Jonsson, B.A., Lindh, C.H., Rylander, L., Rignell-Hydbom, A., Bonde, J.P., Toft, G., 2015. Pregnancy serum concentrations of perfluorinated alkyl substances and offspring behaviour and motor development at age 5–9 years – a prospective study. Environ. Health 14, 2.
Hu, W., Jones, P.D., DeCoen, W., King, L., Fraker, P., Newsted, J., Giesy, J.P., 2003. Alterations in cell membrane properties caused by perfluorinated compounds. Comp. Biochem. Physiol. C Toxicol. Pharmacol. 135 (1), 77–88.
Jiang, Q., 2014. Natural forms of vitamin E: metabolism, antioxidant, and anti-inflammatory activities and their role in disease prevention and therapy. Free Radic. Biol. Med. 72, 76–90.
Johansson, N., Fredriksson, A., Eriksson, P., 2008. Neonatal exposure to perfluorooctane sulfonate (PFOS) and perfluorooctanoic acid (PFOA) causes neurobehavioural defects in adult mice. Neurotoxicology 29 (1), 160–169.
Johansson, N., Eriksson, P., Viberg, H., 2009. Neonatal exposure to PFOS and PFOA in mice results in changes in proteins which are important for neuronal growth and synaptogenesis in the developing brain. Toxicol. Sci. 108 (2), 412–418.
Karrman, A., Ericson, I., van Bavel, B., Darnerud, P.O., Aune, M., Glynn, A., Lignell, S., Lindstrom, G., 2007. Exposure of perfluorinated chemicals through lactation: levels of matched human milk and serum and a temporal trend, 1996–2004, in Sweden. Environ. Health Perspect. 115 (2), 226–230.
Kleszczynski, K., Gardzielewski, P., Mulkiewicz, E., Stepnowski, P., Skladanowski, A. C., 2007. Analysis of structure-cytotoxicity in vitro relationship (SAR) for perfluorinated carboxylic acids. Toxicol. In Vitro 21 (6), 1206–1211.
Kraft, M.L., Weber, P.K., Longo, M.L., Hutcheon, I.D., Boxer, S.G., 2006. Phase separation of lipid membranes analyzed with high-resolution secondary ion mass spectrometry. Science 313 (5795), 1948–1951.
Lee, H.G., Lee, Y.J., Yang, J.H., 2012. Perfluorooctane sulfonate induces apoptosis of cerebellar granule cells via a ROS-dependent protein kinase C signaling pathway. Neurotoxicology 33 (3), 314–320.
Lehmler, H.J., Bummer, P.M., 2004. Mixing of perfluorinated carboxylic acids with dipalmitoylphosphatidylcholine. Biochim. Biophys. Acta 1664 (2), 141–149.
Liao, C., Wang, T., Cui, L., Zhou, Q., Duan, S., Jiang, G., 2009. Changes in synaptic transmission, calcium current, and neurite growth by perfluorinated compounds are dependent on the chain length and functional group. Environ. Sci. Technol. 43 (6), 2099–2104.

Louis, K.S., Siegel, A.C., 2011. Cell viability analysis using trypan blue: manual and automated methods. In: Stoddart, M. (Ed.), Mammalian Cell Viability. Humana Press, pp. 7–12.
Maestri, L., Negri, S., Ferrari, M., Ghittori, S., Fabris, F., Danesino, P., Imbriani, M., 2006. Determination of perfluorooctanoic acid and perfluorooctanesulfonate in human tissues by liquid chromatography/single quadrupole mass spectrometry. Rapid Commun. Mass Spectrom. 20 (18), 2728–2734.
Mariussen, E., Myhre, O., Reistad, T., Fonnum, F., 2002. The polychlorinated biphenyl mixture aroclor 1254 induces death of rat cerebellar granule cells: the involvement of the N-methyl-D-aspartate receptor and reactive oxygen species. Toxicol. Appl. Pharmacol. 179 (3), 137–144.
Mariussen, E., 2012. Neurotoxic effects of perfluoroalkylated compounds: mechanisms of action and environmental relevance. Arch. Toxicol. 86 (9), 1349–1367.
Martin, J.W., Mabury, S.A., Solomon, K.R., Muir, D.C., 2003a. Bioconcentration and tissue distribution of perfluorinated acids in rainbow trout (Oncorhynchus mykiss). Environ. Toxicol. Chem. 22 (1), 196–204.
Martin, J.W., Mabury, S.A., Solomon, K.R., Muir, D.C., 2003b. Dietary accumulation of perfluorinated acids in juvenile rainbow trout (Oncorhynchus mykiss). Environ. Toxicol. Chem. 22 (1), 189–195.
Mosmann, T., 1983. Rapid colorimetric assay for cellular growth and survival: application to proliferation and cytotoxicity assays. J. Immunol. Methods 65 (1–2), 55–63.
Mulkiewicz, E., Jastorff, B., Skladanowski, A.C., Kleszczynski, K., Stepnowski, P., 2007. Evaluation of the acute toxicity of perfluorinated carboxylic acids using eukaryotic cell lines, bacteria and enzymatic assays. Environ. Toxicol. Pharmacol. 23 (3), 279–285.
Myhre, O., Andersen, J.M., Aarnes, H., Fonnum, F., 2003. Evaluation of the probes 2',7'-dichlorofluorescin diacetate, luminol, and lucigenin as indicators of reactive species formation. Biochem. Pharmacol. 65 (10), 1575–1582.
Nilsson, H., Karrman, A., Westberg, H., Rotander, A., van Bavel, B., Lindstrom, G., 2010. A time trend study of significantly elevated perfluorocarboxylate levels in humans after using fluorinated ski wax. Environ. Sci. Technol. 44 (6), 2150–2155.
Nobels, I., Dardenne, F., De Coen, W., Blust, R., 2010. Application of a multiple endpoint bacterial reporter assay to evaluate toxicological relevant endpoints of perfluorinated compounds with different functional groups and varying chain length. Toxicol. In Vitro 24 (6), 1768–1774.
OECD, 2002. Hazard Assessment of Perfluorooctane Sulfonate (PFOS) and Its Salts. http://www.oecd.org/chemicalsafety/risk-assessment/2382880.pdf. (Accessed 29 July 2016).
OECD, 2016. OECD Portal on Perfluorinated Chemicals. https://www.oecd.org/ehs/pfc/. (Accessed 20 July 2016).
Olsen, G.W., Burris, J.M., Ehresman, D.J., Froehlich, J.W., Seacat, A.M., Butenhoff, J.L., Zobel, L.R., 2007. Half-life of serum elimination of perfluorooctanesulfonate, perfluorohexanesulfonate, and perfluorooctanoate in retired fluorochemical production workers. Environ. Health Perspect. 115 (9), 1298–1305.
Reistad, T., Mariussen, E., Ring, A., Fonnum, F., 2007. In vitro toxicity of tetrabromobisphenol-A on cerebellar granule cells: cell death, free radical formation, calcium influx and extracellular glutamate. Toxicol. Sci. 96 (2), 268–278.
Reistad, T., Fonnum, F., Mariussen, E., 2013. Perfluoroalkylated compounds induce cell death and formation of reactive oxygen species in cultured cerebellar granule cells. Toxicol. Lett. 218 (1), 56–60.
Roth, N., Wilks, M.F., 2014. Neurodevelopmental and neurobehavioural effects of polybrominated and perfluorinated chemicals: a systematic review of the epidemiological literature using a quality assessment scheme. Toxicol. Lett. 230 (2), 271–281.
Sato, I., Kawamoto, K., Nishikawa, Y., Tsuda, S., Yoshida, M., Yaegashi, K., Saito, N., Liu, W., Jin, Y., 2009. Neurotoxicity of perfluorooctane sulfonate (PFOS) in rats and mice after single oral exposure. J. Toxicol. Sci. 34 (5), 569–574.
Sayre, L.M., Perry, G., Smith, M.A., 2008. Oxidative stress and neurotoxicity. Chem. Res. Toxicol. 21 (1), 172–188.
Simonian, N.A., Coyle, J.T., 1996. Oxidative stress in neurodegenerative diseases. Annu. Rev. Pharmacol. Toxicol. 36, 83–106.
Xie, W., Bothun, G.D., Lehmler, H.J., 2010a. Partitioning of perfluorooctanoate into phosphatidylcholine bilayers is chain length-independent. Chem. Phys. Lipids 163 (3), 300–308.
Xie, W., Ludewig, G., Wang, K., Lehmler, H.J., 2010b. Model and cell membrane partitioning of perfluorooctanesulfonate is independent of the lipid chain length. Colloids Surf. B Biointerfaces 76 (1), 128–136.
Yu, N., Wei, S., Li, M., Yang, J., Li, K., Jin, L., Xie, Y., Giesy, J.P., Zhang, X., Yu, H., 2016. Effects of perfluorooctanoic acid on metabolic profiles in brain and liver of mouse revealed by a high-throughput targeted metabolomics approach. Sci. Rep. 6, 23963.